APPENDIX A: SAMPLE MAPS AND SPECTRA

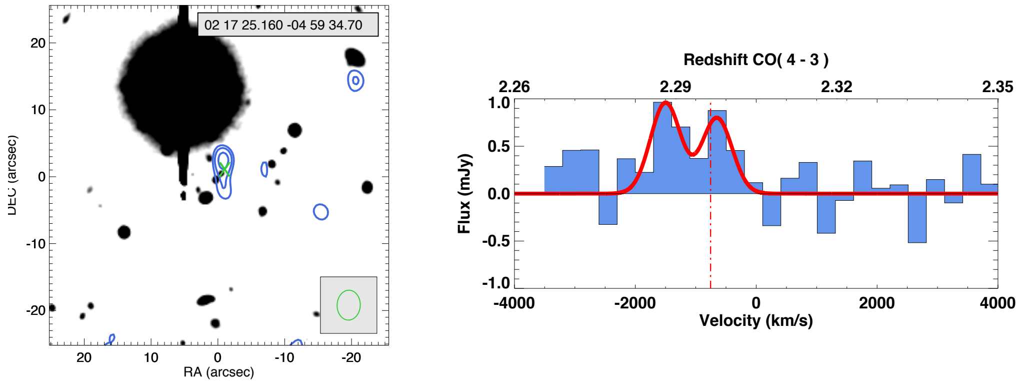

Figure A1. SMM J021725−0459. Note: All maps and spectra in the appendices are displayed identically to this, unless otherwise stated in the respective captions. *Left panel*: Multi-wavelength source map. Blue contours: integrated ^{12}CO image in 1σ steps, starting at 2σ. Red contours: 24μm (where available). The background is a stacked image of all 4 Spitzer IRAC bands (where available; otherwise we have used other near-IR imaging; K-band is shown here). The FWHM of the synthesised beam is shown in the corner, and the green cross indicates the centre of the radio emission. *Right panel*: ^{12}CO spectrum, taken at the point of maximum ^{12}CO flux, with the best fitting Gaussian profile overlaid in red. In the cases where a double-peaked profile provided a superior fit (as described in the text), the best fitting double Gaussian profile is shown. Vertical lines indicate previously obtained redshifts, derived as from the following wavelengths: black dashed line = from UV; red dot-dashed line = from Hα or other nebular emission line; green solid line = PAH. For the sources not detected in ^{12}CO, the spectrum has been taken at phase centre. The SMM J J021725−0459 image has been stretched to account for the bright nearby star. ^{12}CO is detected here at 4.7σ. The 850μm source, SMM J021725−0459 (Coppin et al. 2006), was followed up spectroscopically (Alaghband-Zadeh et al. 2012), detecting Hα as indicated, and the ^{12}CO$(4-3)$ and [CI]$(1-0)$ spectra are published in (S. Alaghband-Zadeh et al. in prep).

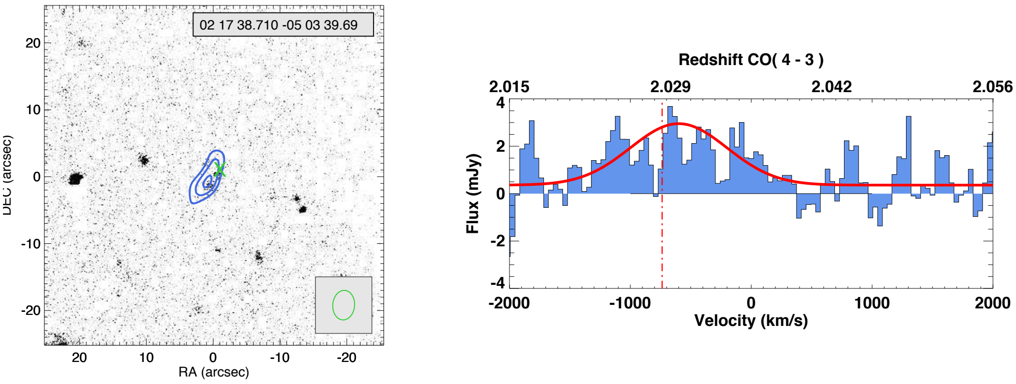

Figure A2. SMM J021738−0503. ^{12}CO is detected at 5.3 σ. The ^{12}CO emission is extended beyond the size of the beam (see inset), so the flux was measured in an aperture around the source. The 850μm source, SMM J021738−0503 (Coppin et al. 2006), was followed up spectroscopically (Alaghband-Zadeh et al. 2012) with Hα derived redshifts for both K-band sources lying under the ^{12}CO contours. The redshift of the northern K-band source is indicated on the ^{12}CO spectrum, the southern source lying +700 km/s offset. The CO($4-3$) and [CI](1-0) spectra are published in (S. Alaghband-Zadeh et al. in prep). Continuum emission is detected at 0.36 ± 0.07 mJy, which compares well to the predicted level of 0.34 mJy (based on simple SED fits to the 850μm flux and far-IR luminosity).

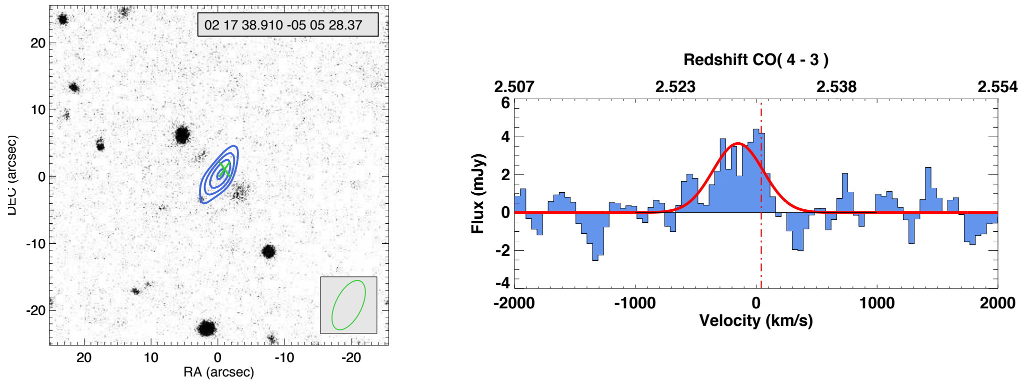

Figure A3. SMM J021738−0505. ^{12}CO is detected at 6.2 σ. The 850μm source, SMM J021738−0505 (Coppin et al. 2006), was followed up spectroscopically (Alaghband-Zadeh et al. 2012), detecting Hα as indicated, and the ^{12}CO(4−3) and [CI](1−0) spectra are published in (S. Alaghband-Zadeh et al. in prep).

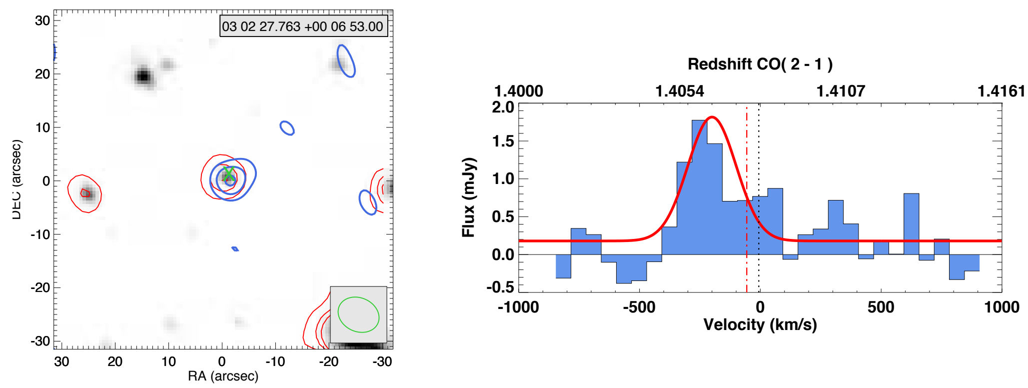

Figure A4. SMM J030227+0006. ^{12}CO is detected at 4.2 σ, and is lined up well with both IRAC and 24μm emission. The PAH redshift is slightly inconsistent, but consistent with $dz \sim 0.02$ redshift fitting errors (Menendez-Delmestre et al. 2007, 2009) ($z = 1.408$ from UV, $z = 1.4076$ from Hα, $z = 1.43$ from PAH). Continuum emission is detected at 0.18 ± 0.05 mJy, higher than the predicted level of 0.09 mJy, but comparable to the 'upper limit', – based on the uncertainty on the far-IR luminosity – of 0.17 mJy.

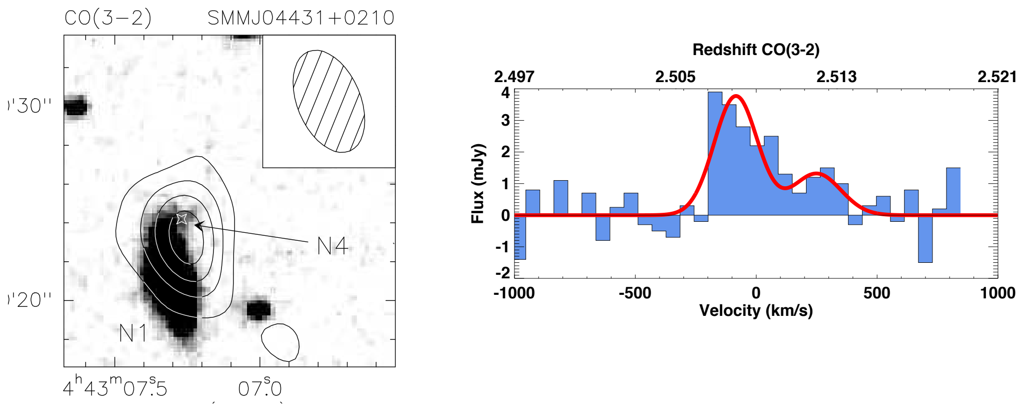

Figure A5. SMM J044315+0210. ^{12}CO is detected at 7.0 σ. This SMG was previously published by Neri et al. (2003); Greve et al. (2005); Tacconi et al. (2006).

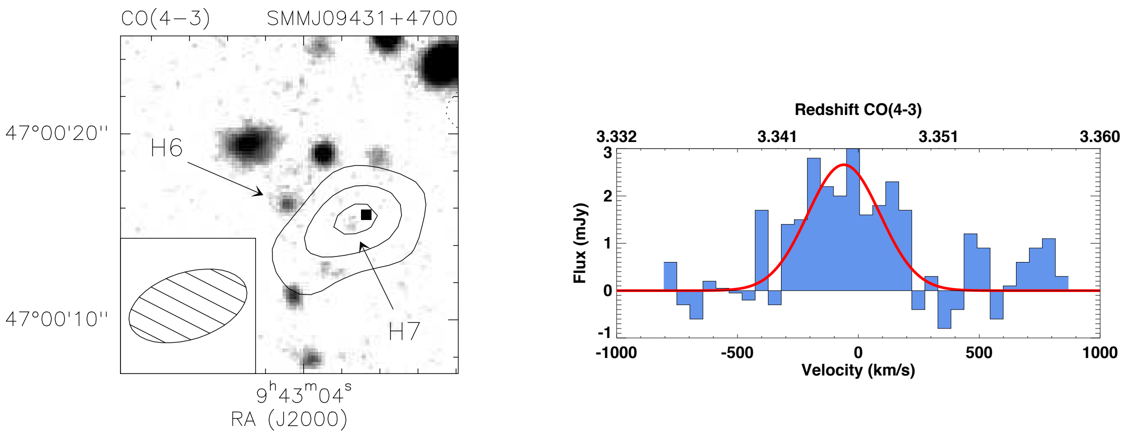

Figure A6. SMM J094304+4700. ^{12}CO is detected at 11.0 σ. This SMG was previously published by Neri et al. (2003); Greve et al. (2005); Tacconi et al. (2006). In Engel et al. (2010), the H6 component of this 30 kpc separated system is also detected at 5σ in ^{12}CO$(6-5)$.

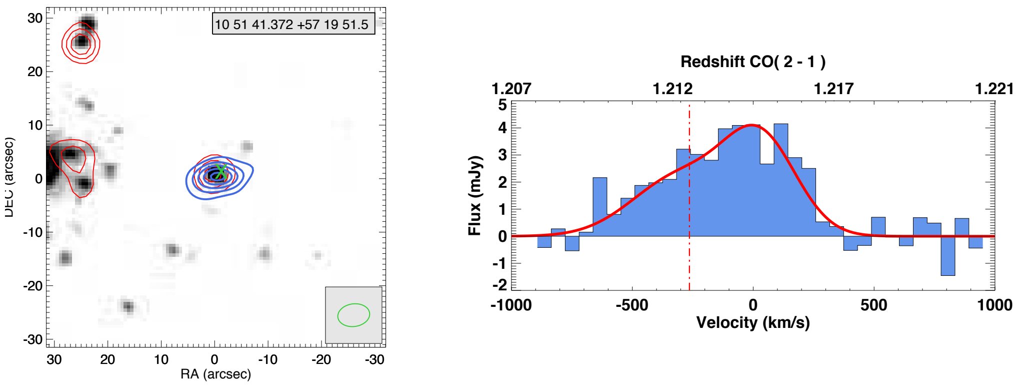

Figure A7. SMM J105141+5719. ^{12}CO is detected at 10.7σ, and contours are shown double spaced (2σ, 4σ, 6σ, etc). The 24μm emission is well aligned with the ^{12}CO. In addition, high spatial resolution (A-config) ^{12}CO($4-3$) data for this SMG is published in Engel et al. (2010), resolving the ^{12}CO into two components.

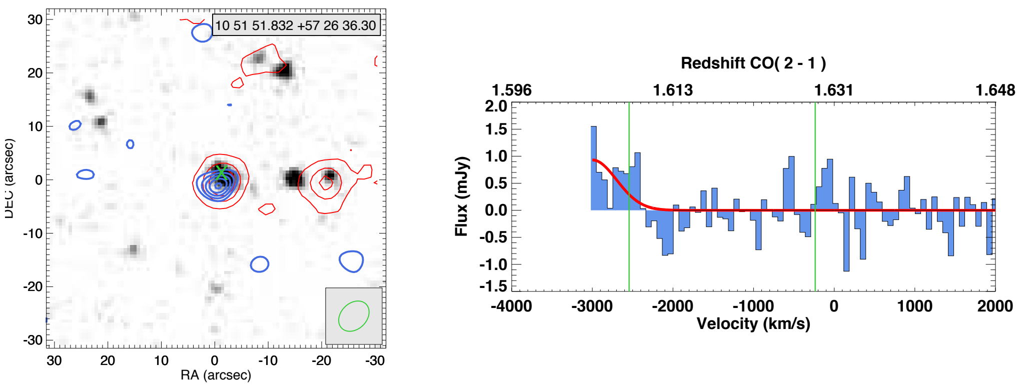

Figure A8. SMM J105151+5726. ^{12}CO is detected at 6.2σ, but near the edge of the bandpass. All emission components are aligned to the radio centre within errors. The published UV-derived redshift, $z = 1.147$ in Ivison et al. (2005) results from a foreground UV-bright galaxy. The PAH redshift can be difficult to constrain in this redshift range, and we show the best two fits – the higher of the two estimates was the initial estimate from Menendez-Delmestre et al. (2009), while the lower estimate is in agreement with the ^{12}CO redshift.

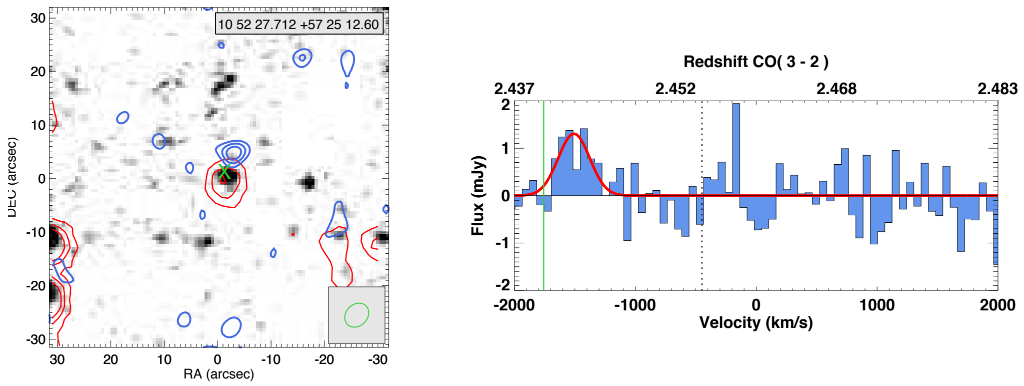

Figure A9. SMM J105227+5725. ^{12}CO is detected at 5.0σ, though it is $\sim$5$''$ north of other emission components.

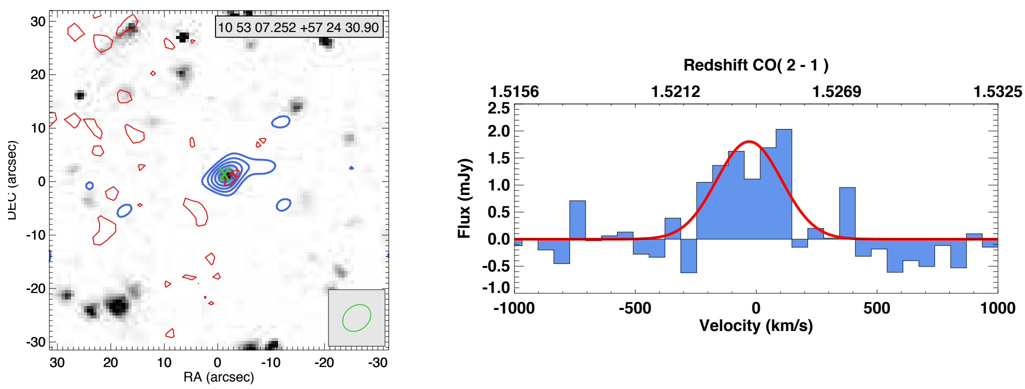

Figure A10. SMM J105307+5724. ^{12}CO is well detected at 6.9σ, and all emission components are close to radio centre. In addition, high spatial resolution (A-config) ^{12}CO(3$-$2) data for this SMG is published in Bothwell et al. (2010), resolving the ^{12}CO into a north-south, 1.5$''$extended source.

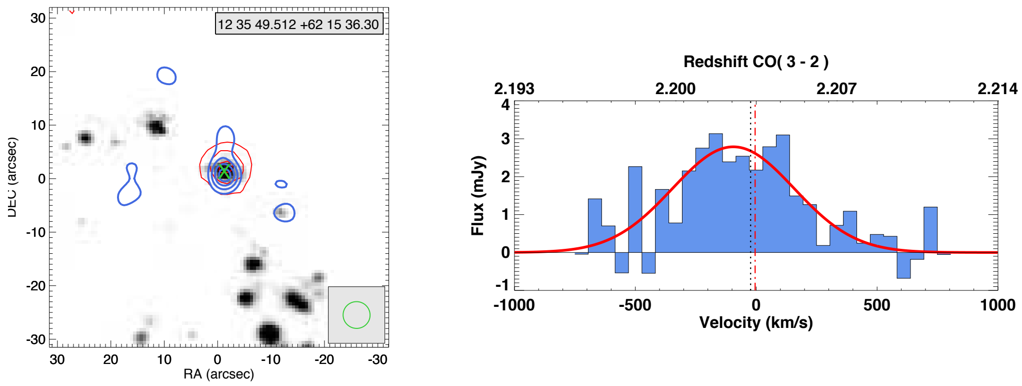

Figure A11. SMM J123549+6215. ^{12}CO contours are double spaced (2σ, 4σ, 6σ, etc). ^{12}CO is well detected at 9.3σ. The PAH redshift is inconsistent with other determinations ($z = 2.203$ from UV, $z = 2.2032$ from Hα; compare to $z = 2.24$ from PAH), slightly larger than the $dz = 0.02$ rms error on the PAH fit. This SMG was previously published by Tacconi et al. (2006).

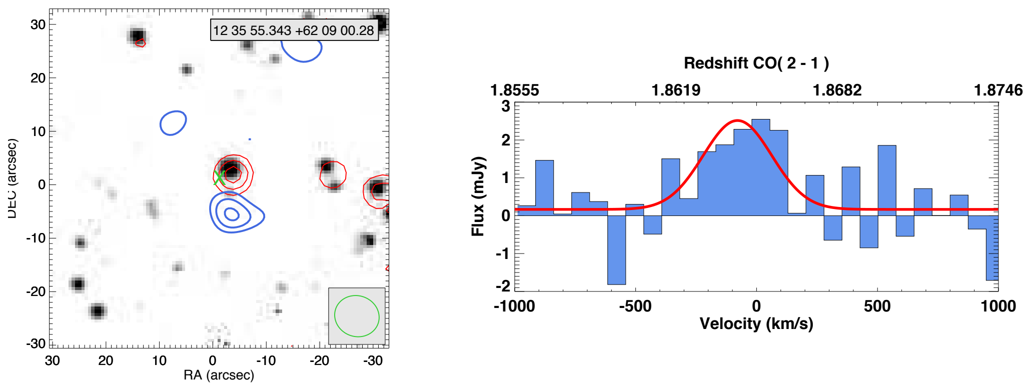

Figure A12. SMM J123555+6209. ^{12}CO is detected at 4.3σ. The peak of emission is between $6''$to $8''$to the south of the IRAC/radio/24μm positions. Both the published Lyα-based UV redshift and the PAH-derived redshift are higher than the ^{12}CO: $z = 1.875$ from UV and $z = 1.88$ from PAH, while the ^{12}CO line is detected at $z = 1.864$. Followup spectroscopic analysis suggests a slightly lower systemic redshift $z = 1.868$ based on weak inter-stellar absorption features blueshifted relative to the Lyα emission line. Continuum emission is detected at 0.16 ± 0.05 mJy, higher than the predicted level of 0.07 mJy, but comparable to the 'upper limit', – based on the uncertainty on the far-IR luminosity – of 0.15 mJy.

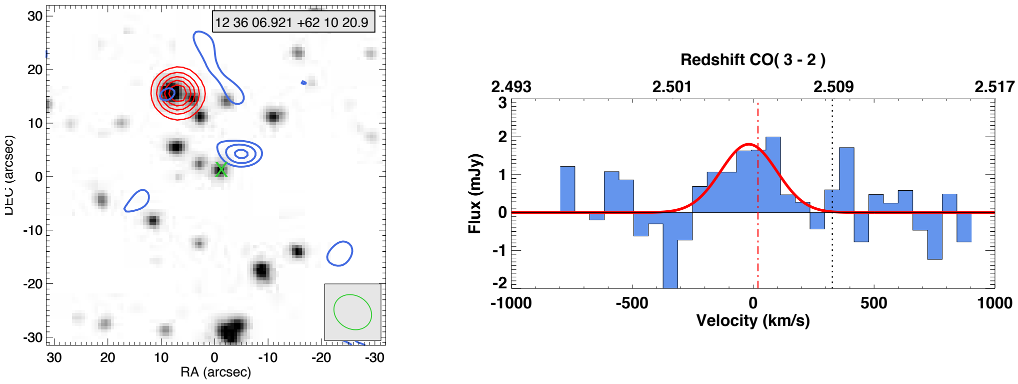

Figure A13. SMM J123606+6210. ^{12}CO is reasonably well detected at 4.3σ (approximately 5$''$to the NE of the radio centre) but there is no apparent near-IR counterpart. A radio source is detected by *Spitzer*-MIPS and IRAC, 20$''$away to the NE, but is likely unconnected with the SMG.

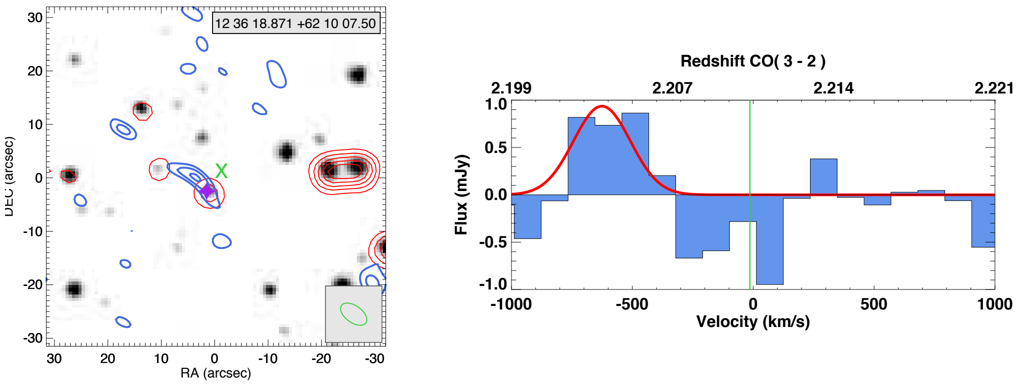

Figure A14. SMM J123618+6210. ^{12}CO is detected at 4.0σ close to the radio centre and within the elongated beam resulting from the poor UV-plane coverage, here marked marked with a purple star. The green cross indicates here the 850μm centre (which was chosen for pointing). We classify this as a candidate detection as in the text, as a result of the offset, ^{12}CO significance, and lack of an optical redshift to verify the PAH.

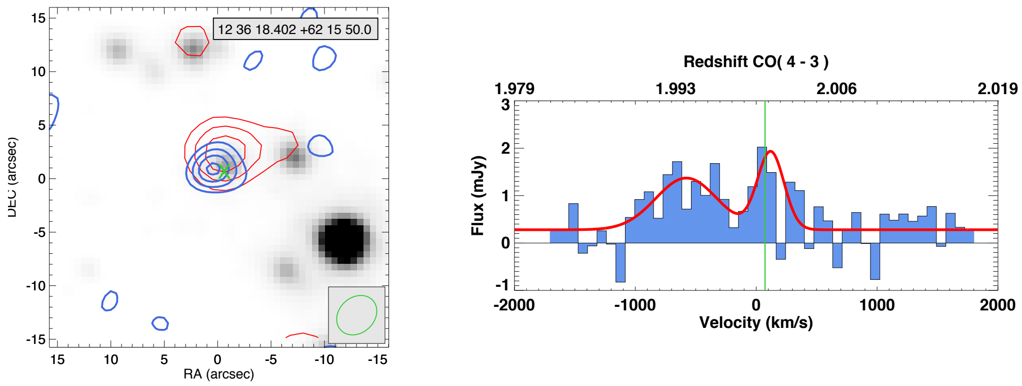

Figure A15. SMM J123618+6215. ^{12}CO contours are double spaced (2σ, 4σ, 6σ, etc). ^{12}CO is strongly detected at 8.6σ and aligned with the 24μm emission. As discussed in Chapman et al. (2009) and Bothwell et al. (2010 – where higher resolution ^{12}CO$(4-3)$ data is published), the redshift originally derived from UV is for the galaxy $0.8''$ to the west, which led to a CO non-detection in a separate observation. Continuum emission is detected at 0.28 ± 0.02 mJy, comparable the predicted level of 0.2 mJy.

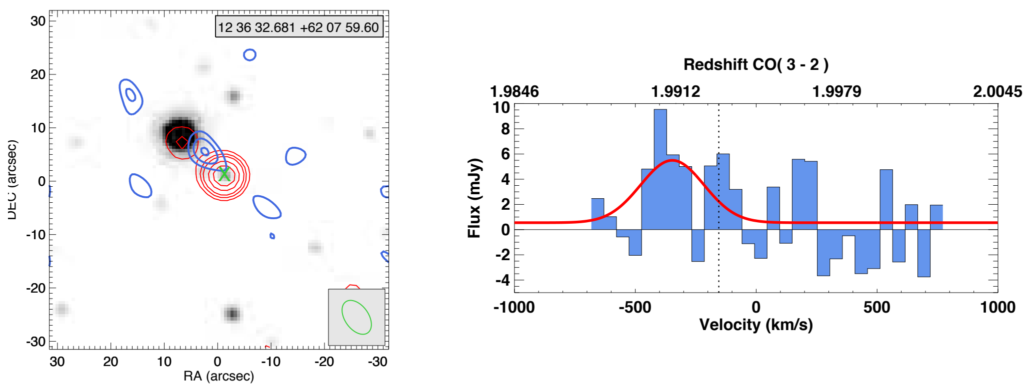

Figure A16. SMM J123632+6208. ^{12}CO emission is detected at 4.5σ, offset by $\sim 7''$ from the radio centre. Continuum emission is detected at 0.51 ± 0.13 mJy, higher than the predicted level of 0.19 mJy, and higher still than the 'upper limit', – based on the uncertainty on the far-IR luminosity – of 0.41 mJy. Based on the large spatial offset, we identify this source as a candidate detection.

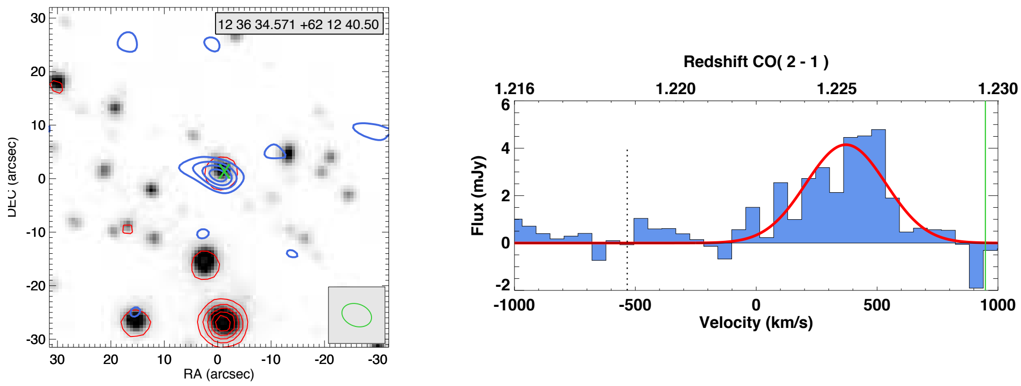

Figure A17. SMM J123634+6212. ^{12}CO contours are double spaced (2σ, 4σ, 6σ, etc). ^{12}CO is strongly detected at 9.5σ. All emission well aligned with the radio counterpart. This source was also observed in ^{12}CO (2–1) by Frayer et al. (2008), who report a ^{12}CO luminosity and FWHM that matches the values reported here. Higher resolution ^{12}CO($6-5$) data was also published in Engel et al. (2010), where they marginally resolve a velocity field within the essentially unresolved source (HWHP 2.2 kpc). Continuum emission is detected at 0.18 ± 0.03 mJy, higher than the predicted level of 0.1 mJy, but comparable to the 'upper limit', – based on the uncertainty on the far-IR luminosity – of 0.22 mJy.

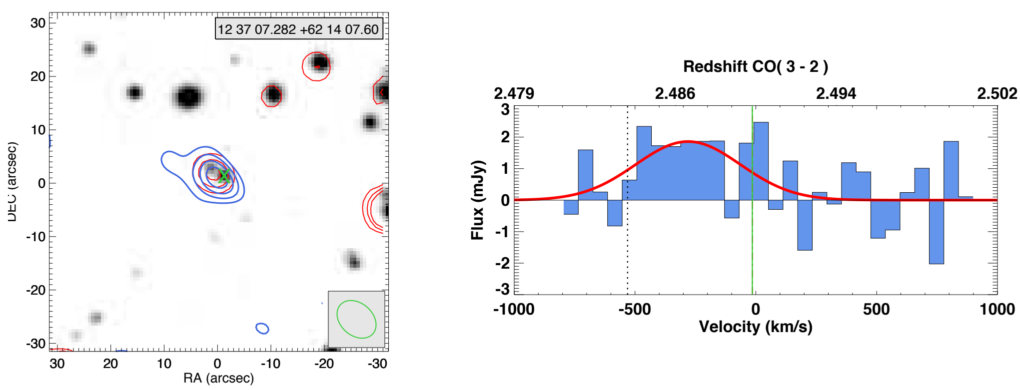

Figure A18. SMM J123707+6214. ^{12}CO is well detected at 5.9σ. All emission components line up well. High resolution imaging (Tacconi et al. 2006, 2008) show this source to consist of two ^{12}CO emission components, separated by $\sim 2.5''$, mirrored by the double radio and IRAC sources.

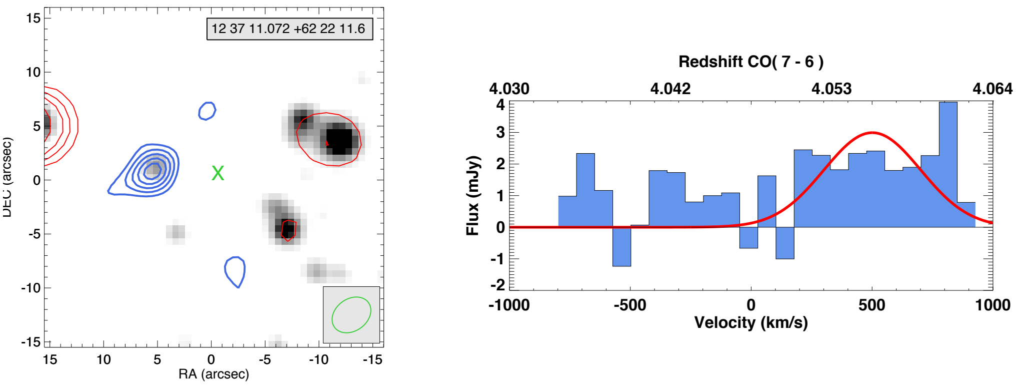

Figure A19. SMM J123711+6222 = GN20. The phase centre (green cross) was chosen to lie between GN20 (east), and GN20.2 (west; not detected). Both galaxies are detected in lower-J imaging (Daddi et al. 2009). The spectrum consists of two lines; ^{12}CO(7–6) (fitted with a Gaussian function), and [CI], approximately 700 km/s bluewards of this. The data was previously presented in Casey et al. (2009), although their overestimated 2mm continuum strength led them to question the detection of the ^{12}CO$(7-6)$ line.

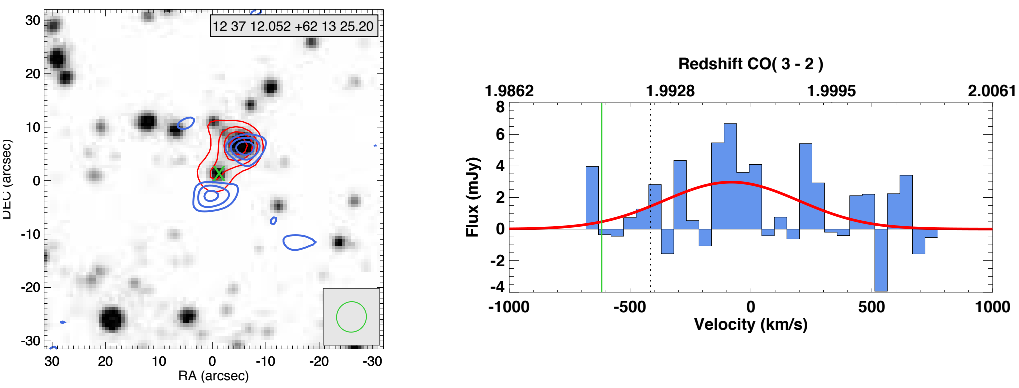

Figure A20. SMM J123711+6213. The ^{12}CO$(3-2)$ detection for this source was originally published by Chapman et al. (2008). The spectrum shown is the NW ^{12}CO source. ^{12}CO is detected at $\sim 4.8\sigma$ – well aligned with radio, 24μm and IRAC emission. The green cross here indicates the phase centre lying between the two ^{12}CO sources (see SMM J123712+6213 below). SMM J123711+6213 is also well detected at higher resolution (A-config) in ^{12}CO$(4-3)$ at $> 6\sigma$, as reported in Bothwell et al. (2010), with lower resolution D-config ^{12}CO$(4-3)$ data presented in Casey et al. (2011).

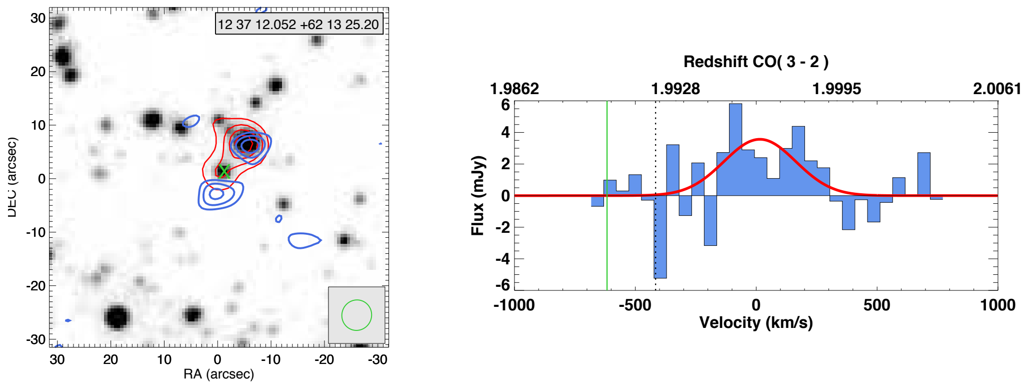

Figure A21. SMM J123712+6213. The spectrum shown is the SE ^{12}CO source. ^{12}CO is detected at $\sim 4.7\sigma$, but the source is offset from $5''$ to the south of the radio position, and the mid-IR IRAC position. However, this source is also detected at 4.5σ in ^{12}CO$(4-3)$ at the same southern offset position, as reported in Bothwell et al. (2010), lending additional weight to the reality of the $5''$ offset.

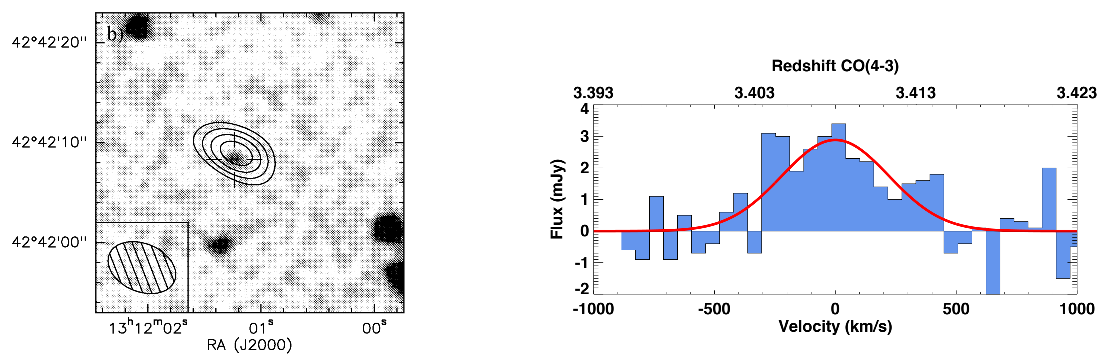

Figure A22. SMM J131201+4242. ^{12}CO is detected at $\sim 5.7\sigma$. The image is taken from Greve et al. (2005). Higher resolution ^{12}CO$(6-5)$ data is published in Engel et al. (2010), resolving the ^{12}CO emission into three components.

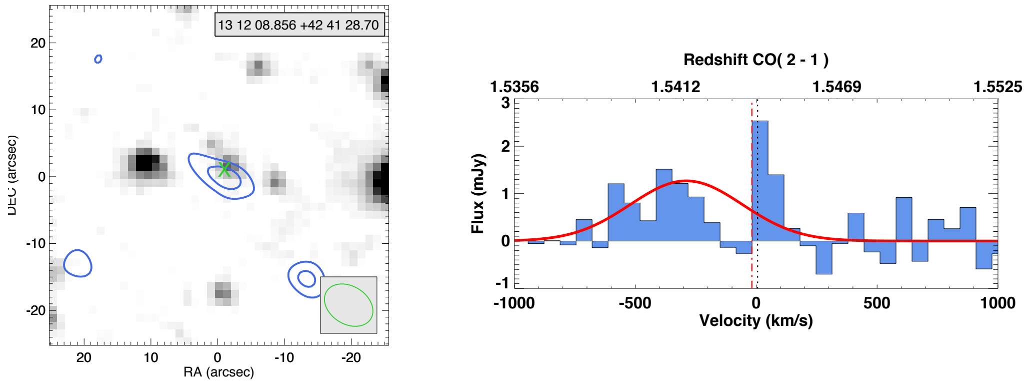

Figure A23. SMM J131208+4241. The source is weakly detected in ^{12}CO at 3.6σ, but is aligned with the radio counterpart, and with the weak IRAC identification where the optical redshifts were measured. We identify this as a candidate detection mainly based on the weak ^{12}CO detection.

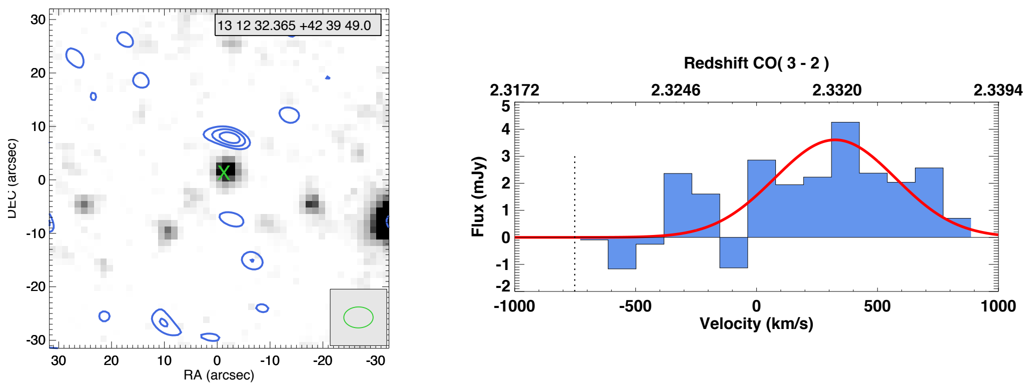

Figure A24. SMM J131232+4239. ^{12}CO is detected at 4.9σ, but is offset to the north by 8″. The Hα redshift (obtained for the radio-identified IRAC source shown) is significantly offset from the ^{12}CO as well – (z = 2.300 from Hα, while z = 2.320 is measured from UV Lyα line, and the ^{12}CO line gives z = 2.332). This source could represent a spatially extended merging system, similar to the SMG complex reported by Ivison et al. (2011). We identify this as a candidate detection based on the large offsets spatially and in velocity.

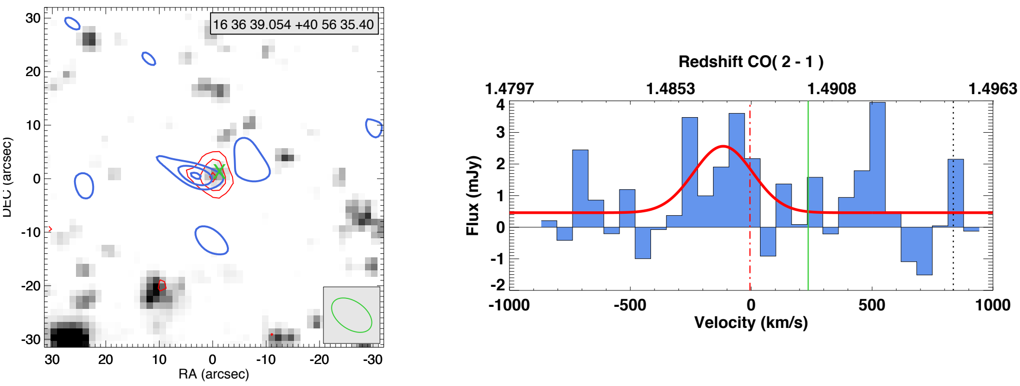

Figure A25. SMM J163639+4056. ^{12}CO is detected at 4.5σ, is offset $6''$ to the east of the radio position, but is consistent within 2σ within the elongated beam shape. We identify this as a candidate detection. Continuum emission is detected at 0.46 ± 0.04 mJy, higher than the predicted level of 0.09 mJy, and higher again than the 'upper limit' – based on the uncertainty on the far-IR luminosity – of 0.2 mJy. However the continuum value is highly uncertain, as a result of the low quality of the spectrum.

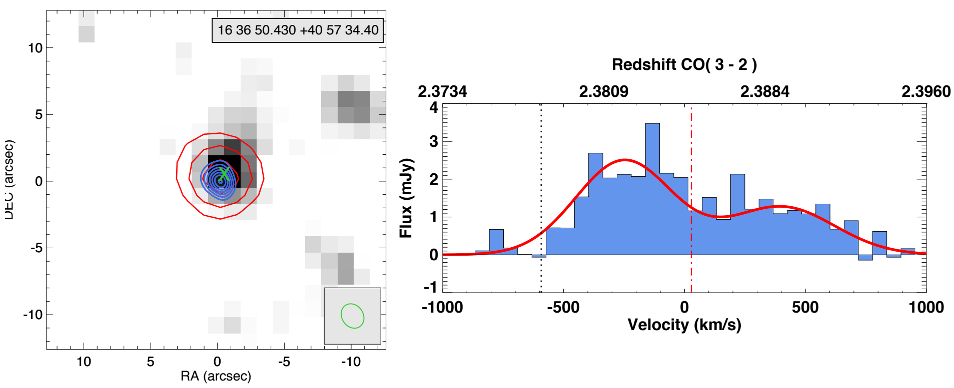

Figure A26. SMM J163650+4057. ^{12}CO is strongly detected at 8.1σ. The source is lined up with 24μm and near-IR emission at the position of the radio counterpart. This is a higher resolution image, and as a result the map size is shown as $25\text{x}25''$. The data was previously published by Tacconi et al. (2006, 2008) along with higher resolution ^{12}CO$(7-6)$ data showing an elongated linear feature.

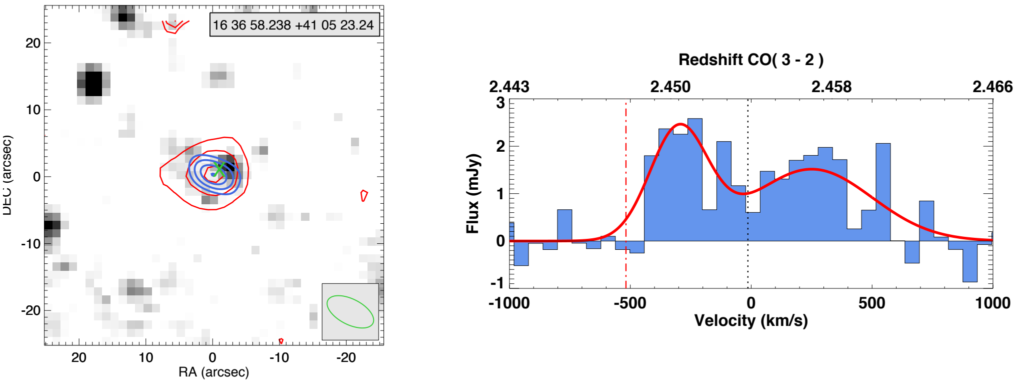

Figure A27. SMM J163658+4105. [12]CO is well detected at 5.0σ. Source is well aligned with 24μm emission. This source was previously published by Greve et al. (2005) and Tacconi et al. (2006, 2008), the higher resolution, higher-J data showing a very compact ^{12}CO(7−6) source (HWHP=0.8 kpc).

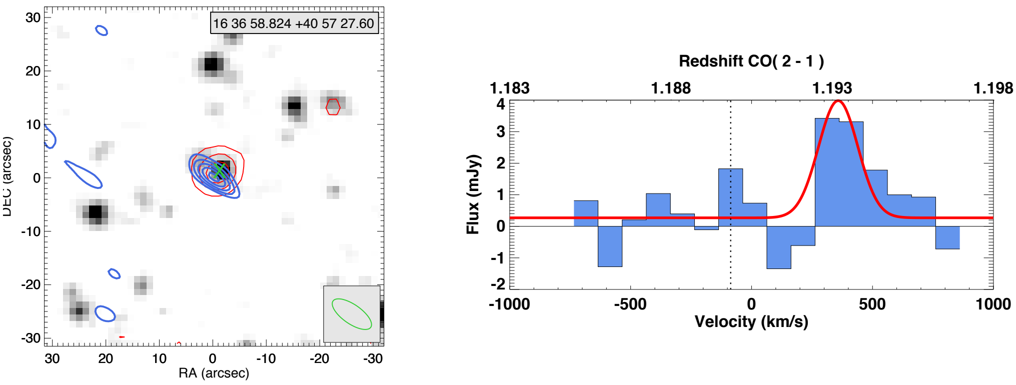

Figure A28. SMM J163658+4057. [12]CO is detected at 6.3σ. The PAH redshift is slightly high, at $z = 1.20$ (but still consistent, given the typical $dz \sim 0.02$ error in fitting PAH features). Continuum emission is detected at 0.27 ± 0.05 mJy, higher than the predicted level of 0.14 mJy, but lower than the 'upper limit', – based on the uncertainty on the far-IR luminosity – of 0.43 mJy.

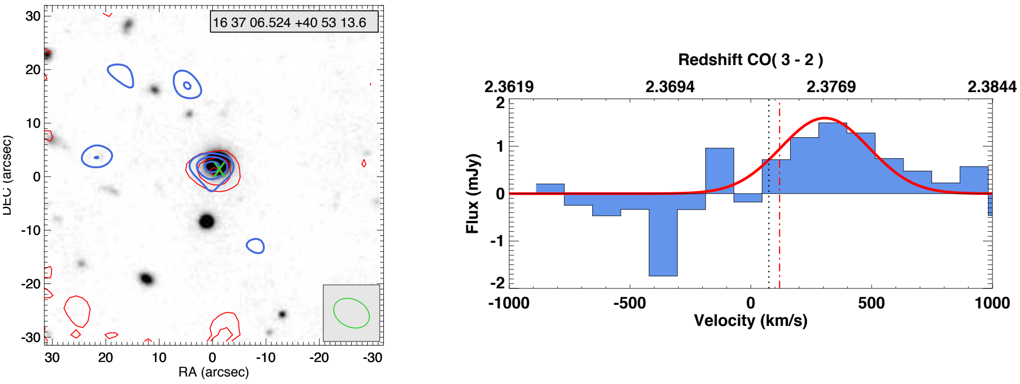

Figure A29. SMM J163706+4053. The background image is I band, rather than a composite IRAC image. ^{12}CO is detected at 4.4σ and aligned with the radio counterpart. The source was previously published in Greve et al. (2005).

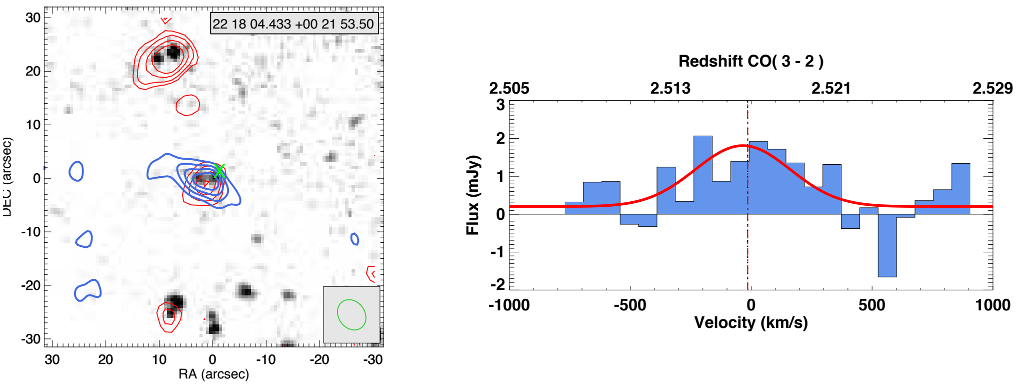

Figure A30. SMM J221704+0021. ^{12}CO detected at 6.0σ, and is lined up with the 24μm emission, and two IRAC sources, both of which are detected in Hα. The ^{12}CO emission is extended beyond the size of the beam (see inset), so the flux was measured in an aperture around the source. The PAH redshift ($z = 2.55$) is slightly inconsistent (Hα and UV give a similar redshift to the ^{12}CO, $z = 2.517$), but again within the typical PAH fitting errors. This source is detected in ^{12}CO (4–3) and in [CI](1-0) in Alaghband-Zadeh et al. (in prep). Continuum emission is detected at 0.20 ± 0.03 mJy, comparable to the predicted level of 0.23 mJy.

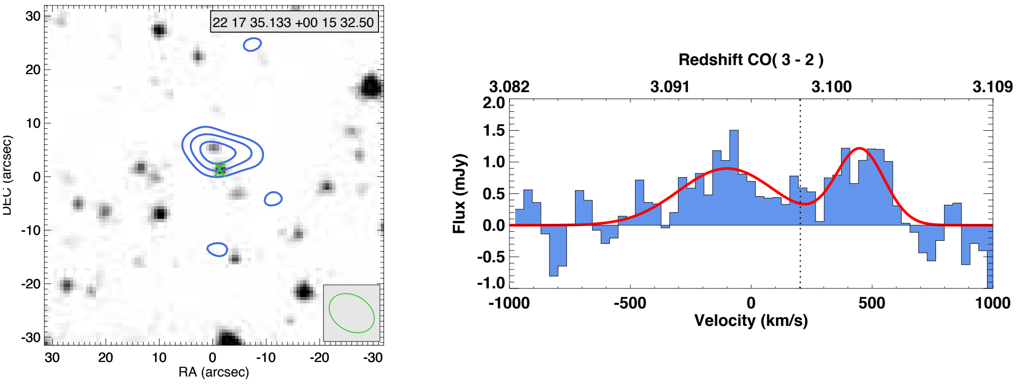

Figure A31. SMM J221735+0015. ^{12}CO is detected at 4.7σ. There is no 24 μm emission associated with this source (Menendez-Delmestre et al. 2009). The PAH redshift ($z = 3.21$) is inconsistent with the ^{12}CO data, however the UV spectrum implies a redshift consistent with the ^{12}CO, $z = 3.098$. The source was previously published in Greve et al. (2005).

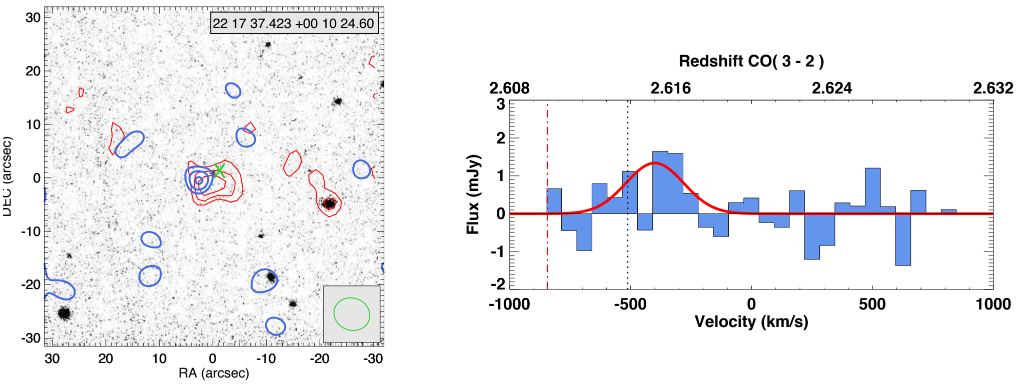

Figure A32. SMM J221737+0010. The background image is K-band. ^{12}CO is detected at 4.2σ, approximately 5" to the east of the radio centre. There is extended 24um over the ^{12}CO region, and a K-band source 3" to the West of the ^{12}CO emission, from which the optical and near-IR spectra were obtained. We identify this as a candidate detection based on the weak ^{12}CO detection and the offset from the optical source.

APPENDIX B: NON-DETECTIONS

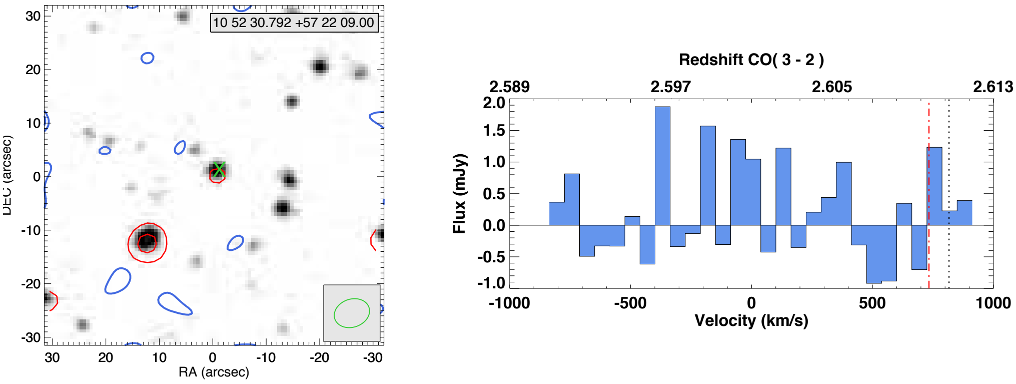

Figure B1. SMM J105230+5722. Non-detection. All the sources shown in Appendix B are true non-detections, which allow useful constraints to be placed on the ^{12}CO flux.

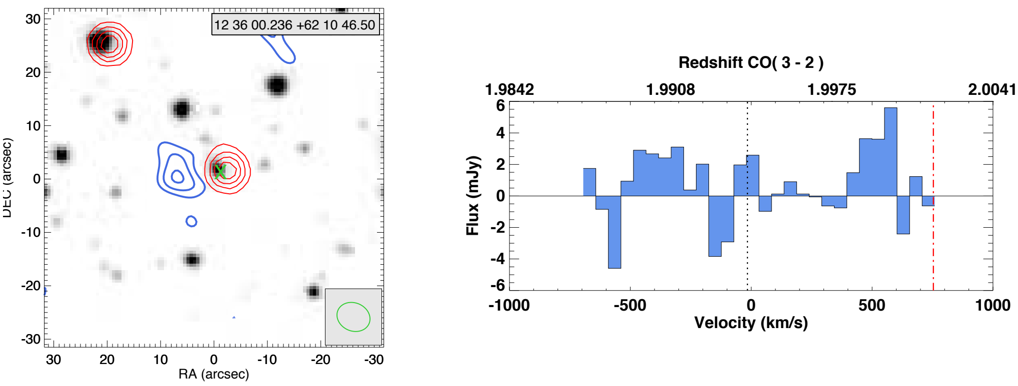

Figure B2. SMM J123600+6210. Non-detection.

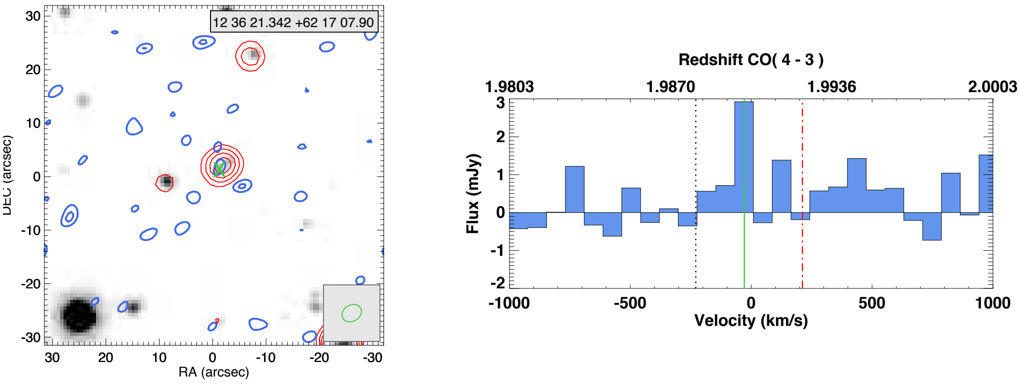

Figure B3. SMM J123621+6217. Non-detection.

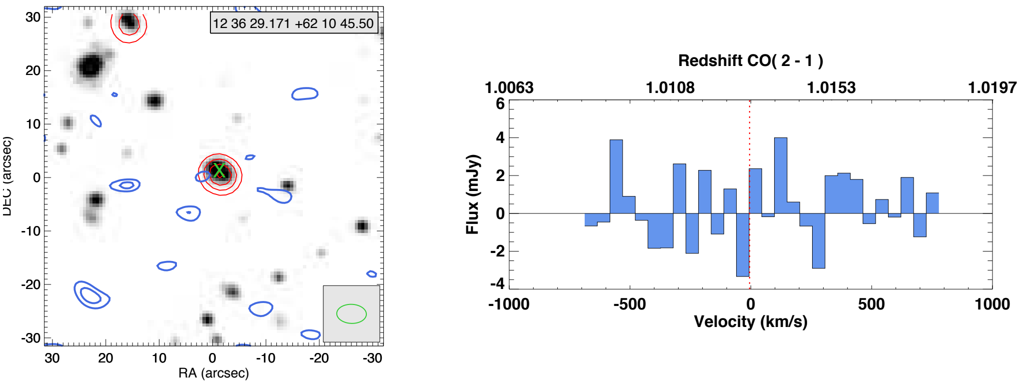

Figure B4. SMM J123629+6210. Non-detection.

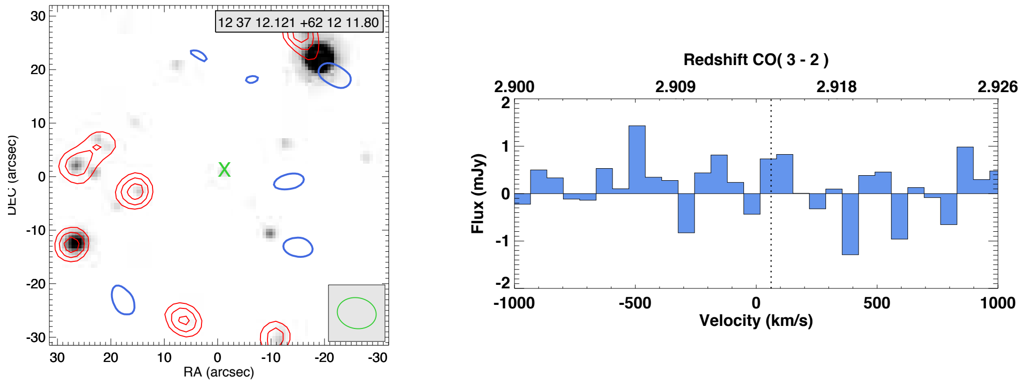

Figure B5. SMM J123712+6212. Non-detection.

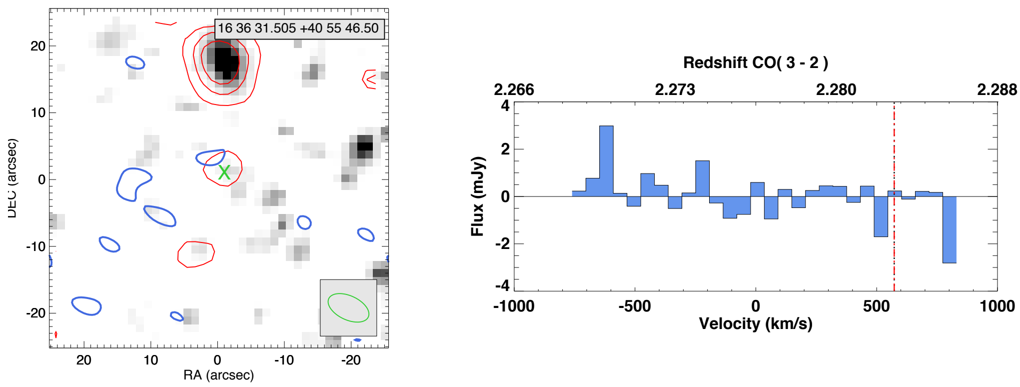

Figure B6. SMM J163631+4055. Non-detection.

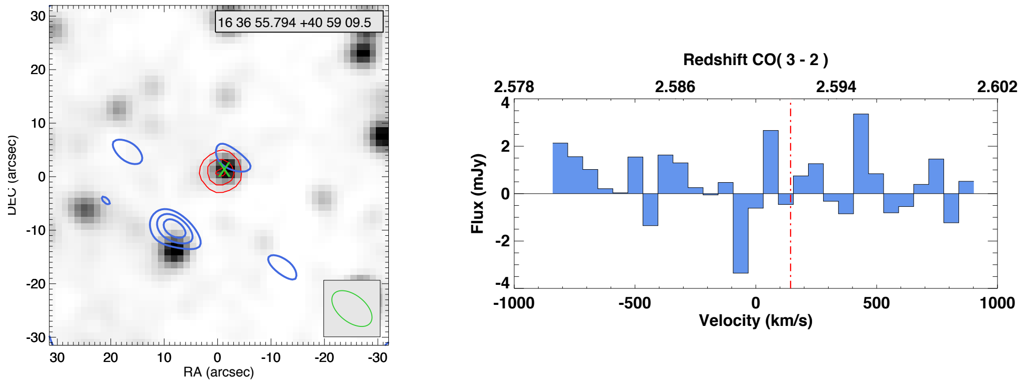

Figure B7. SMM J163655+4059. Non-detection. The emission to the SE of phase centre is most likely spurious, as indicated by IRAC photometric redshift estimates.